Bull. Mater. Sci., Vol. 39, No. 3, June 2016, pp. 857–864. © Indian Academy of Sciences.
DOI 10.1007/s12034-016-1211-1

Ni–Fe–Al_2O_3 electrodeposited nanocomposite coating with functionally graded microstructure

V TORABINEJAD, A SABOUR ROUHAGHDAM, M ALIOFKHAZRAEI* and M H ALLAHYARZADEH

Department of Materials Engineering, Faculty of Engineering, Tarbiat Modares University, P.O. Box 14115-143, Tehran 14117 13116, Iran

MS received 15 June 2015; accepted 21 January 2016

Abstract. **In this study, a Ni–Fe–Al_2O_3 nanocomposite coating was deposited on the substrate of low-carbon steel by electrodeposition from a sulphate-based bath. The effects of frequency and duty cycle were investigated to produce the functionally graded (FG) coating. For this purpose, first, the coatings with duty cycle-decreased method (DDM) were deposited in eight steps from 88 to 11%. At the second step, frequency-increased method (FIM) was utilized from 50 to 6400 Hz during eight steps. Assessing of coatings was carried out by scanning electron microscope (SEM), energy dispersive spectroscopy (EDS), potentiodynamic test, Vickers microhardness test and wear test. Microstructure evaluations gained by SEM and EDS demonstrated that the continuous alterations of duty cycle contribute for manufacturing of FG coatings, so that the maximum particle fraction was in the free surface of the coating and its amount was gradually decreased to the interface. These investigations showed that FIM had no effect on production of graded structure. Corrosion and wear tests indicated high corrosion and wear resistance of DDM coatings in comparison to FIM coatings. Investigating the best coatings obtained from both above methods exhibited 50 and 20% reduction in corrosion current density and wear rate, respectively, for DDM specimen in comparison to FIM sample.**

Keywords. **Ni–Fe–Al_2O_3; nanocomposites; wear resistance; functionally graded; duty cycle; frequency.**

1. Introduction

A particular attention has been focussed on Ni–Fe coating in the recent decades because of its suitable properties. The Ni–Fe coatings have been fabricated by employing various methods, of which electrodeposition is more applicable among them [1–3]. To improve the corrosion and wear properties of Ni–Fe coating significantly, ceramic particles have been proposed and considered. Utilizing the nanoparticles of SiC [4] and Si_3N_4 [3] in the matrix of Ni–Fe coating was investigated and resulted in the corrosion resistance improvement. Generally, nanocomposite coatings fabricated by electrodeposition in comparison to the metallic coatings revealed desirable properties such as electrochemical, mechanical and oxidation properties [5]. The more improvement of these properties depends on plating parameters, electrolyte composition, size and distribution of ceramic particles. The electrodeposition of composite coatings can be performed by direct current (DC), pulse current (PC) and pulse reverse current (PRC) methods [6]. Among these methods, the PC method provides more control on structure and properties. As well as, fabricated coatings by the PC method had better tribologic and corrosion properties than DC ones [7]. Current density is the only variable parameter in DC method. Instead, there are three independent variables in the PC method which are pick current density (i_p), on-time (T_{on}) and off-time (T_{off}) [8]. In the pulse current method, the duty cycle (D.C) corresponds to the percentage of the total on-time of a pulse and frequency is defined as the reverse of total time of a cycle which are given below [9]:

$$\text{D.C} = \frac{T_{on}}{T_{on} + T_{off}},$$

$$f = \frac{1}{T_{on} + T_{off}}.$$

In electrodeposition process, in presence of ceramic nanoparticles which are in the form of suspension in an electrolyte, a negatively charged layer is formed around the cathode. When direct current is applied, the charged layer with certain thickness prevents from reaching the charged ceramic nanoparticles to the electrode surface. In PC method, the current is turned off at specific times to discharge the charged layer around the electrode. This causes the easy entrance of charged ceramic particles into the neighbouring layer of electrode and finally reaching to its surface [10]. However, the use of pulse current can be more useful due to the high existence of ceramic particles. Also, the wide range of properties can be obtained by adjusting the pulse parameters [11]. Employing the capability of the PC, investigators have recently succeeded to apply functionally graded coatings (FG) from a bath by continuous reduction of duty

*Author for correspondence (maliofkh@gmail.com, khazraei@modares.ac.ir)

cycle [12]. The decrease of duty cycle led to increase in volume fraction of nanoparticles in a metallic matrix of FG coating [13]. In this method, a layer with high duty cycle has been deposited first on the substrate surface, and duty cycle decreased in latter layers. Kim *et al* [14] and Lari Baghal *et al* [15] produced functionally graded coatings of Ni–SiC using the current density variation. Orlovskaja *et al* [16] fabricated the same coating through an alteration in turbulent velocity of bath. In this research, turbulence has been developed with the aid of air bubbles within the solution. Obtained coatings had better properties compared to common composite ones and their utilities can be used, wherever the good toughness of sublayers and high wear resistance of upper layers are required.

As explained above, there have been limited studies in the field of nanocomposite coating with Ni–Fe matrix. On the other hand, the effect of Al_2O_3 nanoparticles has been reviewed as a factor to improve the corrosion and wear behaviour of nickel-based coatings [5,7,12]. Moreover, as mentioned in the literature, the increase of volume fraction of Al_2O_3 nanoparticles from interface to the free surface of the coating results in producing high toughness and suitable wear-resistant coatings. Taking the aforesaid facts into consideration, in this study, it was tried to apply FG nanocomposite coatings in the presence of Al_2O_3 nanoparticles in Ni–Fe matrix by pulse electrodeposition. Sulphate-based bath which is more common and has affordable price was utilized. To establish a gradual change in the fraction of nanoparticles within cross-section, capability of continuous changes of duty cycle and frequency was scrutinized. Corrosion and wear tests were employed to assess the above coatings.

2. Experimental

Low-carbon steel was used as a substrate to deposit nanocomposite coatings of Ni–Fe–Al_2O_3. The low-carbon steel was first prepared with sandpaper (numbers 300–1000), then mechanically polished ($R_a \leq 1$ μm) and degreased in methanol for 5 min. Then, samples were dipped in sulphuric acid of 20 vol% for 30 s. All samples after each step was rinsed in deionized water and dried in hot air. Two nickel sheets with a purity of 99.95% as anode and a low-carbon steel sample as cathode were used in plating cell. Dimensions of anodes and cathode were 4×2.5 cm^2. The sulphate bath was utilized and its composition is given in table 1. Deionized water was used to prepare plating bath. Before starting plating, complete distribution of Al_2O_3 nanoparticles in solution was required. For this, the prepared bath was stirred by a magnetic stirrer with a rotating speed of 500 rpm for 12 h, and then subjected to ultrasonic waves with a frequency of 20 kHz and power of 250 W for 30 min. During the plating process, magnetic stirrer with 100 rpm rotating speed and ultrasonic waves with a frequency of 20 kHz and power of 50 W were used.

Every deposited coating in this study consists of eight layers. In the first step of applying FG coating, the first layer was applied with high duty cycle (88%) and in the final layer it was with low duty cycle (11%). This kind of duty cycle application has been adjusted according to the effect of pulse parameters reported previously [13,15], for more adsorption of particles in the coating surface and low fraction in the vicinity of the interface. In the second step, frequency alterations were used to change the volume fraction of particles and it was increased from 50 to 6400 Hz in eight steps. The average applied current density (i_{avg}) from the rectifier was 3 A dm^{-2}, pH for the complete plating process was in the range of 3–3.5, and electrolyte temperature was kept at 50°C. The required time for deposition of each layer was 1500 s and total thickness of coating was approximately 120 μm. The schematic variations of pulse parameters are shown in figure 1. Furthermore, table 2 exhibits i_p values

Table 1. Chemical composition of electrodeposition bath.

Compositions	g l^{-1}
$NiSO_4 \cdot 6H_2O$	250
$NiCl_2 \cdot 6H_2O$	40
H_3BO_3	35
$FeSO_4 \cdot 7H_2O$	50
Saccharin	1
Al_2O_3 nanoparticles	50
Sodiumdodecylsulphate (SDS)	0.5

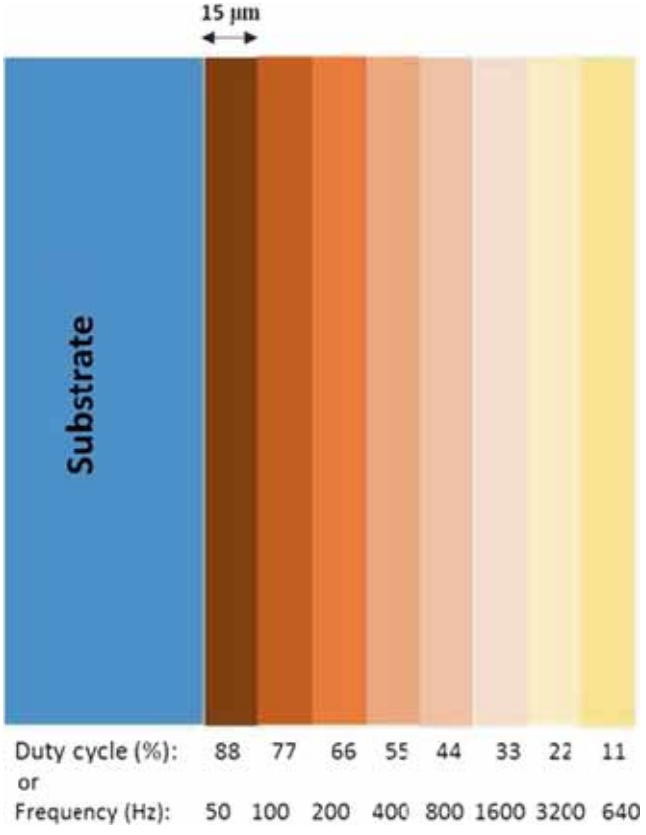

Figure 1. The schematic illustration of regulated pulse parameters for different layers in electrodeposition of Ni–Fe–Al_2O_3 coatings.

Table 2. The used duty cycles and their corresponding pulse peak current (i_p).

Duty cycle (%)	Pulse peak current density (i_p) (A dm^{-2})
11	3.4
22	3.9
33	4.5
44	5.4
55	6.8
66	9.0
77	13.6
88	27.2

corresponding to each duty cycle. The used nanoparticle morphology was investigated by transmission electron microscope JEOL-2010. Scanning electron microscope (SEM) of Zeiss: Sigma/VP equipped to energy dispersive spectroscopy (EDS) was used to investigate microstructural and chemical composition of obtained coatings. Hardness has been measured using Vickers microhardness tester of Buehler Micromet 1. The microhardness measurement was calculated using a 50 g load applied for 15 s. The reported hardness is the average of five different readings. Corrosion test was done by potentiostat/galvanostat EG&G-273A and a three-electrode system in 3.5 vol% NaCl solution. The platinum electrode and saturated calomel electrode (SCE) were utilized as counter and reference electrodes, respectively. The wear resistance was measured by pin-on-disk device in dry condition according to ASTM G-99-95a. The sliding wear test was carried out up to a sliding distance of 250 m. The employed pin was SAE 52100 and curvature radius of its tip was 3.5 mm. The applied force of 40 N and rotation speed of 90 rpm were used in wear test.

3. Results and discussion

3.1 *Microstructure and chemical composition study*

Figure 2 shows the nanoparticle morphology of Al_2O_3 used in this study. Nanoparticles approximately are in spherical form and their average size is 20 nm. The cross-section of two applied coatings by pulse plating is demonstrated in figure 3. Figure 3a indicates the cross-section of Ni–Fe–Al_2O_3 coating which has been electrodeposited by duty cycle-decreased method (DDM) from 88 to 11%. The obtained coating had an approximate thickness of 120 μm and was free of any defects such as crack or pore, and there is no evidence of separation in the interface of the substrate-coating. The higher magnification defined region in figure 3a is shown in figure 3c. This image shows that the most of the particles in the matrix have dimensions of less than 100 nm and, of course, a few of them have the average size more than the initial size of nanoparticles (20 nm). This type of distribution in which the agglomeration has reached to minimum, is more suitable for producing nanocomposite coating. The obtained map of EDS shows that the vol%

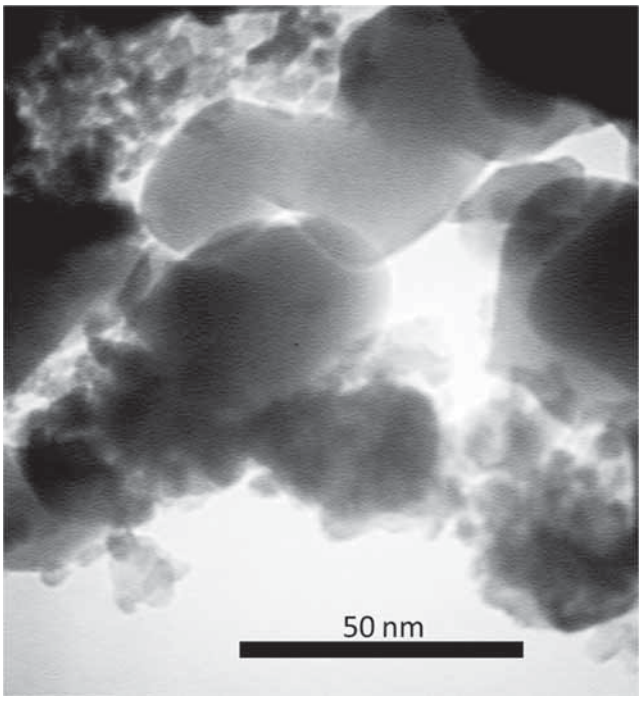

Figure 2. TEM image of Al_2O_3 nanoparticles.

of Al_2O_3 particles are less in the vicinity of the interface, also the amount of it gradually increases with decreasing of duty cycle and has the maximum value in the coating surface. As seen in table 2, the amount of i_p increased by decreasing the duty cycle. Increasing of particles in the surface can be attributed to low duty cycle and high i_p. Such observations are justified with the Guglielmi's model [17]. According to this model, in the first step, physically weak adsorption of particles occurs in the electrode surface, which is most likely surrounded through the thin layer of solvent molecules and adsorbed ions. This thin layer prevents the reaction between particle and electrode. This step is same as the ion adsorption in which the overlapping area of the particle is a function of its concentration in the solution. In the second step, which is electrochemical in nature, strong electrical field separates thin layer around the particle and deposits them in the coating. In this step, particles are irreversibly adsorbed [18]. In general, the occurrence of second step is more difficult than physical adsorption of particles and thus, the latter step which leads to a strong adsorption of particles is a controlling step of deposition speed. Strong adsorption of particles may be stimulated in high overpotential that can be obtained in the high current density [19]. For this reason, the high current density increases volume fraction of particles. In addition to mentioned factor, the duty cycle can increasingly affect the process. A low-duty cycle in the pulse current means that T_{off} is high and the tendency of ceramic particles to introduce double layer increases. Also, at the low T_{on}, particles with larger sizes are less deposited in the metallic matrix [20]. So, the decreasing of duty cycle caused to increase the volume fraction of nanoparticles in the Ni–Fe matrix. Figure 4 presents the cross-sectional image

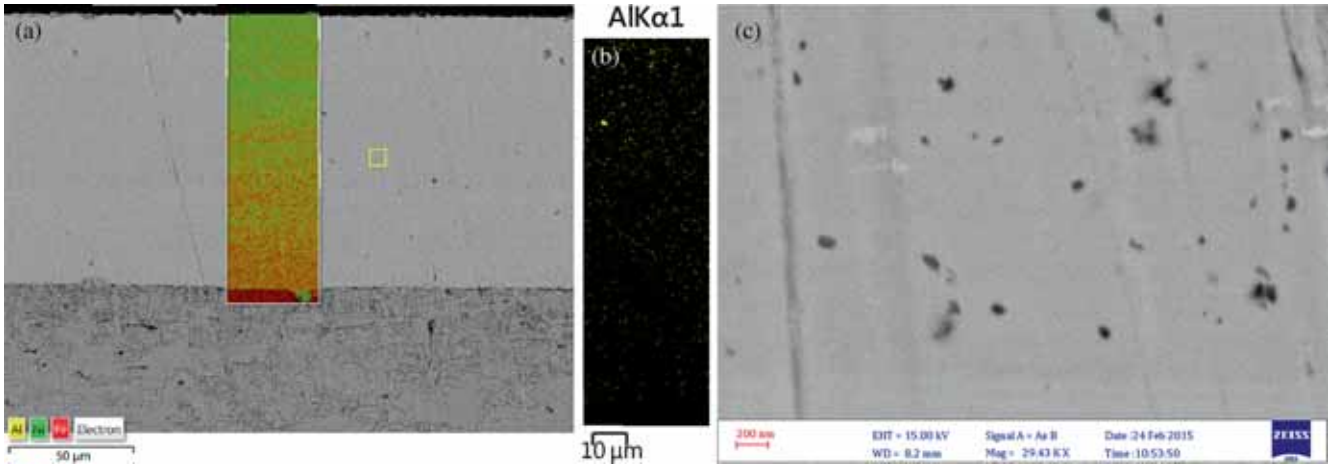

Figure 3. (**a**) The cross-section SEM image of Ni–Fe–Al_2O_3 that was deposited with continuous variation of duty cycle from 88 to 11% at constant frequency of 100 Hz. (**b**) EDS map from indicated section for Al element representing Al_2O_3 particles. (**c**) High magnification image of indicated region.

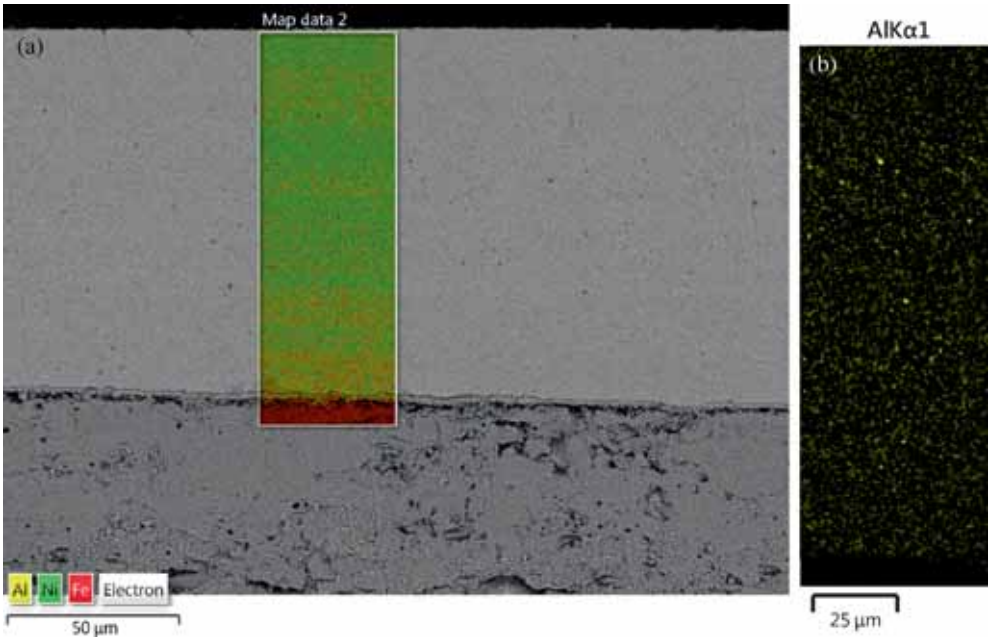

Figure 4. (**a**) The cross-section image of Ni–Fe–Al_2O_3 that was deposited with continuous variation of frequency from 50 to 6400 Hz at constant duty cycle of 44. (**b**) EDS map from indicated section for Al element representing Al_2O_3 particles.

of electrodeposited coatings in the constant duty cycle and frequency-increased method (FIM). Although the FG state in distribution of particles is not observed, the obtained EDS map showed the uniform distribution of ceramic particles. Apparently, there is no effect of pulse frequency on the volume fraction of embedded particles. Whenever the PC electrodeposition is used, mass transfer is being a continuous process by electrolyte stirring, but the load transfer solely carried out in T_{on} [8]. Moreover, in T_{on}, the mobility of free ions to move the surface is more than the mobility of surrounded particles [20]. Hence, a lot of free ions move to the surface, and the amount of particles is not affected. The fraction of alumina nanoparticles for each deposited layer of different FG coatings is revealed in figure 5a. As said, the pulse frequency has not been affected the fraction of nanoparticles. This was in a good agreement with previous results in the case of Ni–Al_2O_3 electrodeposition [12]. The content of nanoparticles in DDM coatings from 0.75 wt% in the vicinity of interface have reached to 1.35 wt% in the last layer in free surface. In FIM specimens, the content of alumina is dependent on duty cycle and is in the range that was achieved for similar layers in DDM. Despite

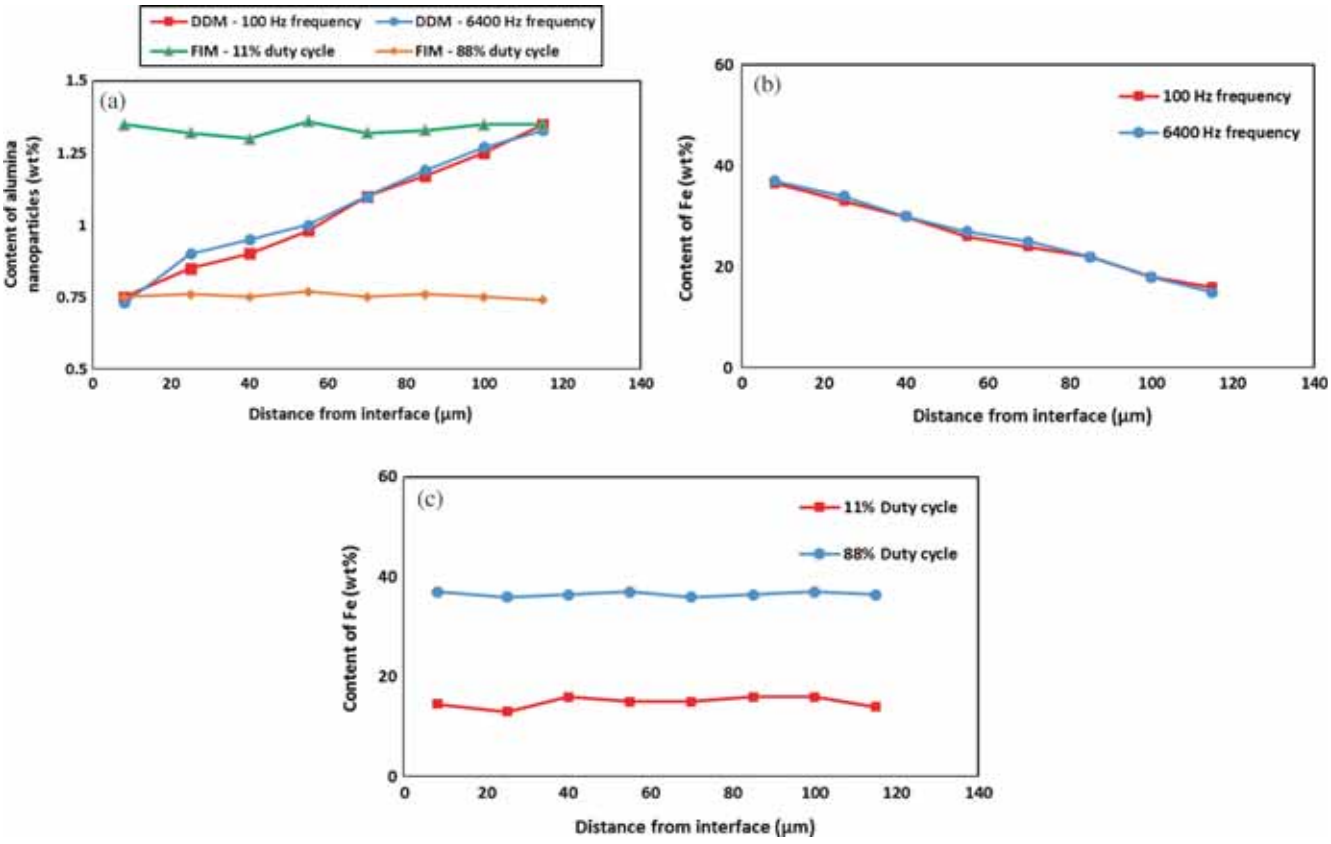

Figure 5. The EDS chemical composition profiles in the cross-section of Ni–Fe–Al_2O_3 coatings: (**a**) content of alumina nanoparticles in the coatings, (**b**) content of Fe in the DDM coatings and (**c**) content of Fe in the FIM coatings.

the above observations, the effect of DDM and FIM on the variation of chemical composition is significant in the matrix of coating. Therefore, the amount of Fe in each layer was measured through point EDS. The amounts of Fe in the coatings produced by DDM are depicted in figure 5b. As the plot demonstrates, the amount of Fe is gradually decreased from the interface of the substrate (37 wt%) and reached to its least value in the coating surface (15 wt%). Such a coating not only prevents the sudden alteration in the interface but also because of better corrosion resistance of Ni, nickel enrichment in upper layers of coating can be advantageous. The other point is independency of chemical composition of matrix from the pulse frequency. As observed, the high frequency of 6400 Hz in DDM specimens have not been affected by the content of Fe. This behaviour has been reported in previous studies for Ni–Fe coatings [1,21]. The point EDS of FIM coatings are plotted in figure 5b. As seen, the variation of chemical composition along the cross-section is negligible and FG state is not observed in the chemical composition of coating matrix. Consequently, in DDM and FIM coatings, the amounts of Fe in the deposited layers by 88 and 11% duty cycles are 37 and 15 wt%, respectively, independent of frequency. The concept of increasing Fe with the decrease of peak current density was mentioned in previous studies and attributed to the anomalous deposition of Fe element [22,23]. The same results have been reported for Ni–Co [24] electrodeposition.

3.2 *Microhardness study*

The results of Vickers microhardness are shown in figure 6 for FG coatings. Microhardness was carried out from a cross-section of coatings in three regions of them, so that the coating considered in three equal sections and microhardness was measured for each section. According to these results, coatings of DDM have high hardness, whereas their hardness is being decreased within the cross-section from free surface to the vicinity of the substrate–coating interface. Basically, when a ceramic hard phase introduces into a metallic matrix, it causes to increase composite hardness due to two reasons: Orovan and Hall–Petch effects. Hard particles can either inhibit grain boundary movement in the metallic matrix or grain growth during the coating process (Hall–Petch effect). More the number of hard particles are, the more number of dislocations will be locked. On the other hand, the required stress for movement of locked dislocation between two particles will be increased based on the Orovan effect [25]. Presence of finer particles decreases the mobility of grain boundaries, because of the enhancement of inter-phase interfaces [19]. Accordingly, increasing of hardness near the free surface can be ascribed to high Al_2O_3 particle fraction on the upper layers. In FIM coatings, the variation of hardness does not follow a specific trend, and the amount of it in cross-section almost remained unchanged. Such a state is

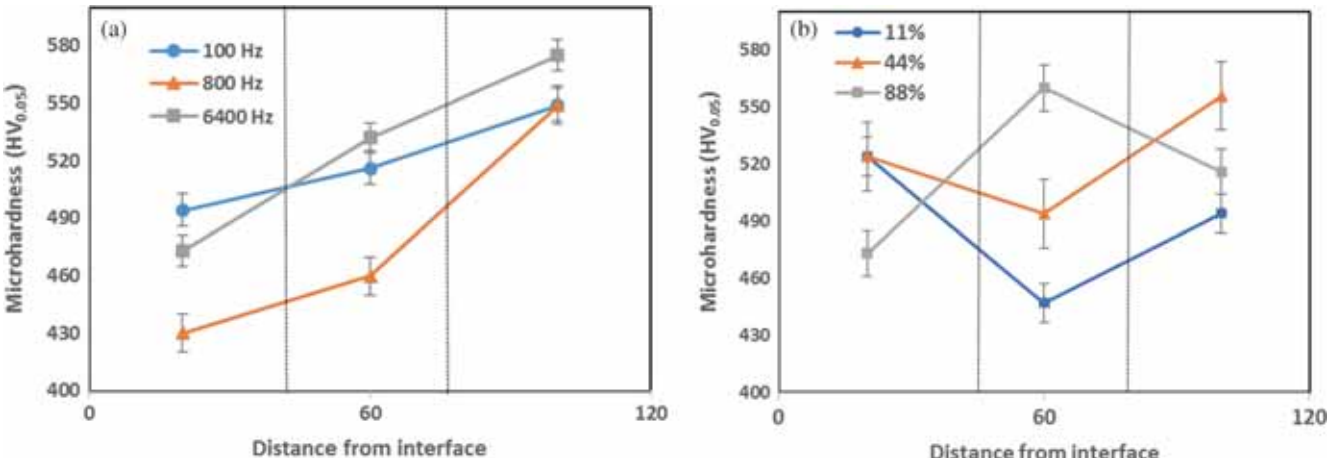

Figure 6. Results of Vickers microhardness test for Ni–Fe–Al_2O_3 coatings deposited by (**a**) DDM at various frequencies and (**b**) FIM at various duty cycles.

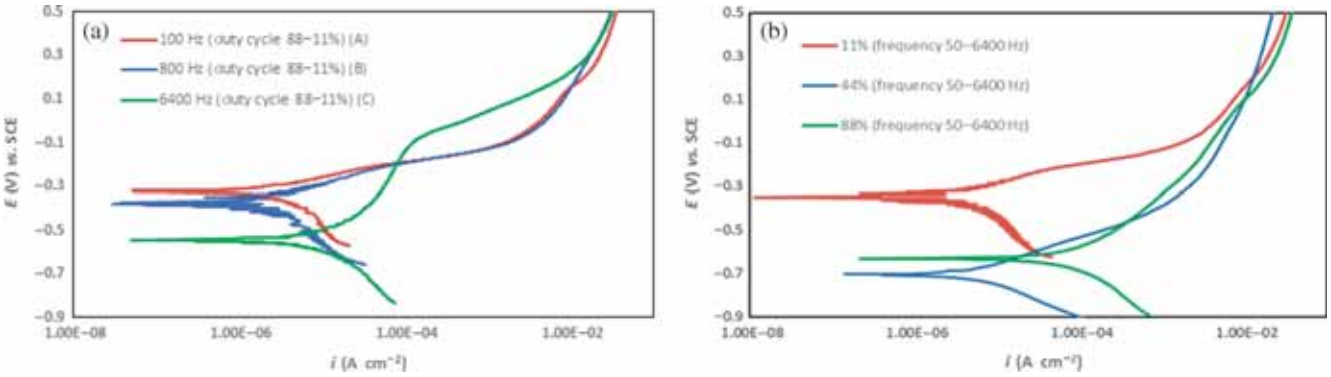

Figure 7. Potentiodynamic polarization curves of Ni–Fe–Al_2O_3 coatings obtained by (**a**) DDM and (**b**) FIM.

expected due to the lack of changes in the particle fraction of the coating.

3.3 *Corrosion study*

The results of potentiodynamic tests are shown for the coating of Ni–Fe–Al_2O_3 in figure 7. The amounts of corrosion potential (E_{corr}) and corrosion current density (i_{corr}) have been obtained by drawing tafel slopes for these curves presented in table 3. Generally, the outcomes of potentiodynamic tests exhibit that the DDM coatings have higher corrosion resistance than FIM. Also, comparison of the highest corrosion resistance in each group of samples show that there is a 50% decrease in i_{corr} in the sample A than D. Figure 7a shows that the increase of frequency contributes to the displacing of corrosion potential of the DDM coating to the more active amounts, so that this value from −313 mV (SCE) in the applied coating with a frequency of 100 Hz has been decreased to –546 mV (SCE) in 6400 Hz. Previous studies represent that increasing the pulse frequency leads to finer structures in metallic [26] and nanocomposite [27] coatings. Indeed, more the frequency is, the smaller are T_{on} and T_{off}. In the beginning of pulse plating, new nuclei which are formed in T_{on} period has no adequate time to growth, so, immediately, T_{off} is started and leads to a fine-grained structure. In such a structure, due to the presence of many number of grain boundaries, the rapid diffusion routes are prepared for the corrosive ones. On the other land, these locations (grain boundaries and triple junctions) are active locations, which by rising their density, the number of prone locations for corrosion increases [28]. Figure 7b shows the results of corrosion test for nanocomposite coatings of FIM. The particle distribution in such samples is similar to the samples that are indicated in figure 4. Results of corrosion test for these kinds of coatings show that the increase in duty

Table 3. Corrosion characteristics of Ni–Fe–Al_2O_3 extracted from potentiodynamic polarization curves presented in figure 7.

Sample	A	B	C	D	E	F
β_a (mV per decade)	52	68	67	61	40	116
β_c (mV per decade)	61	105	60	70	60	108
E_{corr} (mV *vs.* SCE)	−313	−366	−546	−344	−444	−633
i_{corr} × 1E6 (A cm^{-2})	0.77	0.92	2.29	1.54	2.42	3.12

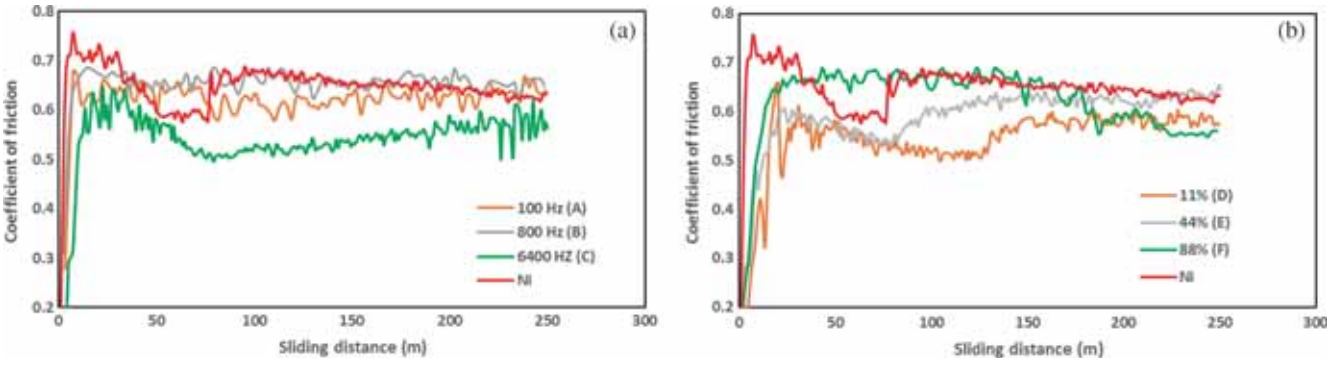

Figure 8. Comparison of coefficient of friction *vs.* sliding distance for Ni–Fe–Al_2O_3 coatings electrodeposited by (**a**) DDM at various frequencies and (**b**) FIM at various duty cycles.

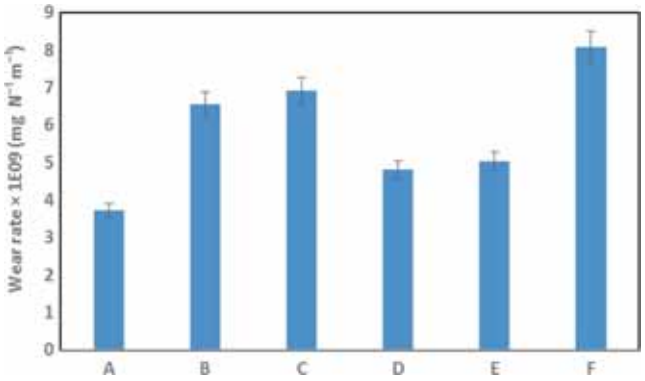

Figure 9. The wear rate results for different samples of Ni–Fe–Al_2O_3 coatings presented in figure 8.

cycle decreases E_{corr}. By increasing duty cycle from 11 to 88%, the i_{corr} has been doubled. Microstructure investigations and chemical composition demonstrated that in duty cycle of 11%, the amount of Fe has 15 wt% and it reaches to 37% by increasing the amount of duty cycle to 88%. Raising of Ni content which is more noble metal than Fe can be considered as a factor of better corrosion resistance in applied coatings with 11% duty cycle. On the other hand, the results of this research and many previous studies showed that the decrease of the duty cycle and increase of plating current density lead to rising the fraction of ceramic particles in the nanocomposite coatings [29]. The presence of ceramic particles in coating improves corrosion resistance in several ways. These particles are barriers against the corrosive species and do not allow more diffusion of these corrosive agents [30]. Furthermore, presence of nanoparticles removes some of the defects and discontinuities between the grains and leads to a high quality and smooth coating [31]. The last reason is a decrease of metallic surface subjected to corrosion in the nanocomposite coatings [32]. Taking into account of these descriptions, increasing of nanoparticle fraction as well as the raising of Ni in the matrix due to duty cycle reduction is the main efficacious criteria on the increase of corrosion resistance of FIM coatings.

3.4 *Wear study*

Figure 8 shows the results of pin-on-disk test comprising the effects of frequency and duty cycle on the wear behaviour of obtained Ni–Fe–Al_2O_3 coatings. It is observed that the coefficient of friction of FG coatings first increased by the rising of sliding distance and reached to a maximum point. Then, this behaviour gets a steady state after a small loss. Enhancement of frequency in FG coatings results in decreasing the average friction coefficient. As described in previous paragraphs, getting a finer structure is the result of frequency increasing. The reduction of friction coefficient with a finer structure has been reported in Ni coatings [33]. Coefficient of friction *vs.* sliding distance for FIM coatings have been presented in figure 8b. Decreasing of duty cycle in such coatings caused the reduction of average friction coefficient. This decrease may be attributed to the increasing of embedded particles as explained in last sections. Raising the fraction of hard nanoparticles on the surface decreases the contact area between abrasive body and alloy matrix. Such a behaviour has been observed in the fabrication of nanocomposite coatings of Ni–SiC too [34]. The wear rates of above samples have been plotted in figure 9. As is obvious, the wear rate is increasing by rising the frequency in the DDM samples. Due to the high content of embedded nanoparticles in low duty cycle, the wear rate is decreased by reducing the duty cycle in FIM samples. This behaviour seems to be reasonable. The best possible states in terms of wear rate for DDM and FIM coatings are A and D samples, respectively. This comparison exhibits that the wear rate has approximately 20% reduction in DDM coating. It is expected that chemical composition, grain size and volume fraction of embedded nanoparticles gradually vary from interface to the free surface in DDM coating [35]. As illustrated in figure 3, the amount of Al_2O_3 particles is decreased in the vicinity of the interface and the Fe content reaches from 37 wt%, in the nearness of interface, to 15 wt% on the surface. So, these coatings have a good compatibility in the interface region with substrate compared to the FIM. Additionally, existence of rich layer of Al_2O_3 particles on the surface which has higher wear resistance rather than sublayers which could have high wear resistance. Such an effect has

been observed in FG coatings of Ni–Co–SiC fabricated by Lari Baghal *et al* [34].

4. Conclusion

In this research, Ni–Fe–Al_2O_3 coating was deposited on the substrate of low-carbon steel by utilizing pulse electrodeposition. Frequency and duty cycle continuously varied in eight steps and FG coatings have been produced by using these variations. The obtained results of this study are mentioned below:

(1) The continuous alterations of duty cycle from 88 to 11% in DDM coatings were contributed in the fabrication of FG coatings, so that the particle fraction has the highest amount in the vicinity of the free surface and the lowest value in the nearness of the interface. As well as, the amount of Fe was 15 wt% in the vicinity of free surface and 37 wt% in the interface.

(2) The incremental variation of frequency from 50 to 6400 Hz in FIM specimens did not change the chemical composition of the matrix and the fraction of trapped nanoparticles.

(3) The Vickers microhardness was higher in the vicinity of free surface of DDM coatings than its amount in the nearness of interface. This occurrence has been attributed to the higher embedded nanoparticles on the surface compared to the vicinity of interface region.

(4) The wear and corrosion resistance of DDM coatings were better than FIM ones and the best obtained coatings of these two states, values of i_{corr} and wear rate for DDM coating compared to FIM had 50 and 20% reductions, respectively.

References

[1] Sanaty-Zadeh A, Raeissi K and Saidi A 2009 *J. Alloys Compd.* **485** 402

[2] Su C-W, He F-J, Ju H, Zhang Y-B and Wang E-L 2009 *Electrochim. Acta* **54** 6257

[3] Yusrini M and Idris Y I 2013 *Adv. Mater. Res*. **647** 705

[4] Ataee-Esfahani H, Vaezi M R, Nikzad L, Yazdani B and Sadrnezhaad S K 2009 *J. Alloys Compd.* **484** 540

[5] Chang L, Liu J and Zhang R 2011 *Mater. Corros.* **62** 920

[6] Arunsunai Kumar K, Paruthimal Kalaignan G and Muralidharan V S 2013 *Ceram. Inter.* **39** 2827

[7] Chang L M, An M Z, Guo H F and Shi S Y 2006 *Appl. Surf. Sci.* **253** 2132

[8] Chandrasekar M S and Pushpavanam M 2008 *Electrochim. Acta* **53** 3313

[9] Sajjadnejad M, Mozafari A, Omidvar H and Javanbakht M 2014 *Appl. Surf. Sci.* **300** 1

[10] Alper M, Aplin P, Attenborough K, Dingley D, Hart R, Lane S *et al* 1993 *J. Magn. Magn. Mater.* **126** 8

[11] Low C, Wills R and Walsh F 2006 *Surf. Coat. Technol.* **201** 371

[12] Lajevardi S A, Shahrabi T and Szpunar J A 2013 *Appl. Surf. Sci.* **279** 180

[13] Lajevardi S A, Shahrabi T, Szpunar J A, Sabour Rouhaghdam A and Sanjabi S 2013 *Surf. Coat. Technol.* **232** 851

[14] Kim S K and Yoo H J 1998 *Surf. Coat. Technol.* **108** 564

[15] Lari Baghal S M, Amadeh A and Heydarzadeh Sohi M 2012 *Mater. Sci. Eng. A* **542** 104

[16] Orlovskaja L, Periene N, Kurtinaitiene M and Bikulčius G 1998 *Surf. Coat. Technol.* **105** 8

[17] Guglielmi N 1972 *J. Electrochem. Soc.* **119** 1009

[18] Wang S-C and Wei W-C J 2003 *Mater. Chem. Phys.* **78** 574

[19] Kasturibai S and Kalaignan G P 2014 *Mater. Chem. Phys.* **147** 1042

[20] Bahrololoom M E and Sani R 2005 *Surf. Coat. Technol.* **192** 154

[21] Yin K-M, Jan S-L and Lee C-C 1997 *Surf. Coat. Technol.* **88** 219

[22] Yin K-M and Jan S-L 1996 *Surf. Coat. Technol.* **79** 252

[23] Kieling V C 1997 *Surf. Coat. Technol.* **96** 135

[24] Chung C K and Chang W T 2009 *Thin Solid Films* **517** 4800

[25] Pogrebnyak A D, Shpak A P, Azarenkov N A and Beresnev V M 2009 *Physics-Uspekhi* **52** 29

[26] Youssef K M S, Koch C C and Fedkiw P S 2004 *Corr. Sci.* **46** 51

[27] Goldasteh H and Rastegari S 2014 *Surf. Coat. Technol.* **259** 393

[28] Ovid'ko I 2005 *Inter. Mater. Rev.* **50** 65

[29] Aliofkhazraei M, Ahangarani S and Rouhaghdam A S 2010 *Rare Metals* **29** 209

[30] Bakhit B and Akbari A 2012 *Surf. Coat. Technol.* **206** 4964

[31] Praveen B M and Venkatesha T V 2008 *Appl. Surf. Sci.* **254** 2418

[32] Sajjadnejad M, Omidvar H, Javanbakht M, Pooladi R and Mozafari A 2014 *Trans. IMF* **92** 227

[33] Wasekar N P, Haridoss P, Seshadri S K and Sundararajan G 2012 *Wear* **296** 536

[34] Lari Baghal S M, Heydarzadeh Sohi M and Amadeh A 2012 *Surf. Coat. Technol.* **206** 4032

[35] Choi I, Dao M and Suresh S 2008 *J. Mech. Phys. Solids* **56** 157